Received: 19 December 2020 | Revised: 25 January 2021 | Accepted: 30 January 2021

DOI: 10.1002/eom2.12086

RESEARCH ARTICLE

EcoMat FUNCTIONAL MATERIALS FOR GREEN ENERGY AND ENVIRONMENT WILEY

Generalized Weisskopf-Wigner model of triboelectroluminescence

Lok C. Lew Yan Voon[1] | **Javier E. Hasbun**[1] | **Morten Willatzen**[2] | **Zhong L. Wang**[2]

[1]University of West Georgia, Carrollton, Georgia

[2]Beijing Institute of Nanoenergy and Nanosystems, Chinese Academy of Sciences, Beijing, China

Correspondence
Morten Willatzen, Beijing Institute of Nanoenergy and Nanosystems, Chinese Academy of Sciences, Beijing, China.
Email: morwi@fotonik.dtu.dk

Abstract

The phenomenon of triboelectroluminescence is studied using a generalization of the Weisskopf-Wigner model of spontaneous emission in an electronic two-level system. An irreversible and exponential transfer of charge results from the model. The charge transfer between two linear atomic chains is computed as a function of the separation of the two chains and as a function of the temperature. Triboelectroluminescence due to spontaneous emission is found to be more efficient when the electron states in the two materials have a larger energy separation and decays rapidly with separation. It is insensitive to temperature variation when the electrons emanate from insulators or surface states, but not when they emanate from partially-filled bands due to the thermal excitation of the electrons.

KEYWORDS

contact electrification, spontaneous emission, two-band tight-binding model

1 | INTRODUCTION

The generation of electrostatic charge via contact of or friction between two materials is known as triboelectricity and is a natural phenomenon with important technological and industrial applications.[1,2] Long-time consequences of triboelectric charging include lightning and the operation of laser printers. Even more exciting are the endless possibilities a small-scale, clean and environmental source of energy would bring to self-powered devices and vehicles such as self-powered displays[3] and biosensors.[4,5] A fully quantitative computation of the charge transfer for most macroscopic objects is impossible due to their unknown microstructures and the often ill-defined environmental conditions of experiments.[6] Additionally, the resulting surface charge density of the order of 10^{-4} cm^{-2} amounts to roughly one unit of charge transferred for every 100 000 or so of surface atoms.[7] Hence, most theories and modeling to date have concerned themselves with phenomenological approaches.[8,9] Certainly, if the charged particles being transferred are electrons, as is most often the case, a fundamental starting point should be a quantum theory of the electrons. Electronic-structure theories of material properties, as implemented in ab initio codes, have indeed been used to calculate the charge transfer between two materials, albeit with limited success.[10-18] Thus, they were used to compute intrinsic localized molecular-ion levels to validate charge transfer for metal-polymer[10] and polymer-polymer[11] contacts. More recently, they have been used in an attempt to calculate charge transfer, though in some cases the computed quantity was a bond polarity, and in all cases the driving force was not explicity given. A different perspective was recently proposed by Alicki

and Jenkins,[19] whereby the irreversibility of the electron transfer was analyzed in terms of the motion-induced population inversion and this provided an upper bound on the attainable voltage difference.

A resurgence of interest in the study of triboelectricity due to better experimental control using nanostructures and the proposal of a triboelectric nanogenerator (TENG)[1] has led us to propose a different approach to analyzing the charge transfer during the triboelectric process,[20-22] one that can hopefully bridge the different time and length scales of the problem. In References 21 and 22, we studied the charge transfer due to quantum tunneling between two semi-infinite materials and between two linear chains, whereas in Reference 20, we considered a two-level electronic system in thermal equilibrium with a photon bath and the emission of photons accompanying the charge transfer. We label the latter phenomenon as triboelectroluminescence to distinguish from triboluminescence[23] since the latter is often associated with a more complex process. For instance, triboluminescence has been associated with piezoelectric crystals and their symmetry whereas no such requirements are needed to describe triboelectroluminescence.

In this article, we propose a more in depth study of the phenomenon of triboelectroluminescence. The electrons in the two materials are modeled using a one-electron Hamiltonian in a localized basis in order to allow for nonperiodicity. The spontaneous emission process is modeled by generalizing the Weisskopf-Wigner model of spontaneous decay for a two-level atom.[24] The neglect of stimulated emission is justified if there is no photon bath available. Experimentally, this would occur if the system is not enclosed in a cavity, allowing the emitted photons to radiate away and not reach equilibrium in the surrounding of the system. Since the operation of a TENG involves the relative motion of two materials, we have calculated the charge transfer as a function of the separation of the two materials. Furthermore, as experiments have been carried out as a function of temperature in order to elucidate the mechanism of charge transfer, we have investigated the impact of temperature dependence via the Fermi-Dirac function.

2 | GENERALIZED WEISSKOPF-WIGNER MODEL

The Weisskopf-Wigner model treats the transition of an electron from an excited atomic state to a ground state with the spontaneous emission of photons and was initially applied to the hydrogen atom. It led to an exponential decay of the electron from the excited state and to a Lorentzian spectrum of emitted photons. We have generalized the above model to study the transfer of electrons from one material (left) to another (right) with the emission of photons.

2.1 | Hamiltonian

The Hamiltonian of the problem represents electrons in the materials interacting with the electromagnetic field:

$$H = H_{\text{elec}} + H_F + H_{\text{int}}, \tag{1}$$

where H_{elec} is a one-electron Hamiltonian, H_F is the Hamiltonian of the transverse electromagnetic field, and H_{int} will be chosen to be a dipole interaction. In order to incorporate materials lacking translational symmetry (ie, finite ones), we choose a Wannier representation of the electron Hamiltonian[25]:

$$H_{\text{elec}} = \sum_{ij,\alpha\beta}\left[\varepsilon_{i\alpha}c^{\dagger}_{i,\alpha}c_{i,\alpha}\delta_{ij}\delta_{\alpha\beta} + \left(t_{i\alpha,j\beta}c^{\dagger}_{i,\alpha}c_{j,\beta} + t^{*}_{i\alpha,j\beta}c^{\dagger}_{j,\beta}c_{i,\alpha}\right)\right], \tag{2}$$

where $c^{\dagger}_{i,\alpha}(c_{i,\alpha})$ creates (annihilates) an electron at site i and with orbital ϕ_α, $\varepsilon_{i\alpha}$ are the onsite energies, and the $t_{i\alpha,j\beta}$ are hopping parameters between two different atoms. We will typically let α represent s- and p-like Wannier orbitals (ie, a two-band model) and only include nearest-neighbor hopping.

The field Hamiltonian H_F is

$$H_F = \sum_{\mathbf{k},s}\hbar\omega_{\mathbf{k}}\hat{n}_{\mathbf{k},s}, \tag{3}$$

where $\hbar\omega_{\mathbf{k}}$ is the photon energy, $\hat{n}_{\mathbf{k},s}$ is the number operator, and $\mathbf{k}$ and s denote the wave vector and polarization, respectively.

The electron-photon interaction representing spontaneous emission between two electronic eigenstates (m denoting a higher energy ("excited") state on the left and n a lower energy state ("ground") on the right) is given by

$$H_{\text{int}} = -\sum_{m,n}\sum_{\mathbf{k},s}\hbar g^{m,n}_{\mathbf{k},s}\hat{\sigma}_{e_m g_n}\hat{a}_{\mathbf{k},s} + \text{h.c.}, \tag{4}$$

where $\hat{\sigma}_{e_m g_n} = e^{\dagger}_m g_n$, with $e^{\dagger}_m$ the creation operator for an electronic excited state m on the left, g_n the annihilation operator for an electronic ground state n on the right, $\hat{a}_{\mathbf{k},s}$ the annihilation operator for a photon, and the coupling constant is

$$g_{\mathbf{k},s}^{m,n} = i\sqrt{\frac{\omega_{\mathbf{k}}}{2\hbar\varepsilon_0 V}}\mathbf{d}_{m,n}\cdot\varepsilon_{\mathbf{k},s}, \tag{5}$$

with V the field normalization volume, $\mathbf{d}_{m,n}$ the electric dipole matrix element coupling states e_m and g_n,

$$\mathbf{d}_{m,n} = \langle g_n|e\mathbf{r}|e_m\rangle,$$

and $\varepsilon_{\mathbf{k},s}$ the photon polarization.

2.2 | Wave function

Each material is assumed to consist of discrete energy states, with the left material populated with electrons up to a certain energy state (at $T = 0$ K), the "excited" states, and the right material having empty states of lower energy, the "ground" states, in order to accommodate those electrons. When the electron is on the left, we assume it is coupled with no photon, whereas it is coupled to one photon of wave vector $\mathbf{k}$ and polarization s when it is in the ground state. Thus, a general state of an electron at a time t is given by the wave function

$$|\psi(t)\rangle = \sum_m a_m(t)e^{-i\omega_m t}|e_m,0\rangle + \sum_n b_n(t)e^{-i\omega_{\mathbf{k},s}t}|g_n,1_{\mathbf{k},s}\rangle. \tag{6}$$

Here, $\hbar\omega_m$ is the energy of the electron in the excited state with respect to the ground-state energy.

2.3 | Schrödinger equation

The time dynamics of the electrons is obtained by solving the time-dependent Schrödinger equation:

$$H|\psi(t)\rangle = i\hbar\frac{\partial|\psi(t)\rangle}{\partial t}. \tag{7}$$

Our problem is more general than the two-level system considered by Weisskopf and Wigner since there are multiple electronic levels in each material. However, we can arrive at a solution resembling the Weisskopf-Wigner (WW) solution[26] by first considering one level (labeled m and n, respectively) in each material. Then, the WW solution applies and one can immediately write

$$\frac{da_m(t)}{dt} = -\frac{\Gamma}{2}a_m(t), \quad \Gamma = \frac{\omega_0^3|d_{mn}|^2}{3\pi\varepsilon_0\hbar c^3}, \tag{8}$$

where $\hbar\omega_0 = (E_m - E_n)$ and d_{mn} are the energy difference and the electric dipole between the two electronic states, respectively. The WW differential equation can be trivially integrated to give a decaying exponential evolution with time. If we write each energy eigenstate as a linear combination of the Wannier orbitals,

$$|e_m\rangle = \sum_{i,\alpha} c_{i,\alpha}^{m,L}\phi_{i,\alpha}, \; |g_n\rangle = \sum_{j,\beta} c_{j,\beta}^{n,R}\phi_{j,\beta}, \tag{9}$$

one can re-express the band dipoles in terms of atomic dipoles:

$$|d_{mn}|^2 = \left|\sum_{ij,\alpha\beta} c_{i,\alpha}^{m,L^*}c_{j,\beta}^{n,R}\left\langle\phi_{i,\alpha}\middle|\mathbf{er}\middle|\phi_{j,\beta}\right\rangle\right|^2. \tag{10}$$

Next, we consider multiple left states and a single right state n. Then, the differential equations for the a_m's and for b_n are

$$\frac{da_m(t)}{dt} = i\sum_{\mathbf{k},s} g_{\mathbf{k}}^{m,n}b_{n\mathbf{k}}(t)e^{-i(\omega_{\mathbf{k}}-\omega_{mn})t}, \tag{11}$$

$$\frac{db_{n\mathbf{k}}(t)}{dt} = i\sum_{m'} g_{\mathbf{k}}^{m',n^*}a_{m'}(t)e^{i(\omega_{\mathbf{k}}-\omega_{m'n})t}. \tag{12}$$

Following the procedure of Weisskopf and Wigner, we find

$$\frac{da_m(t)}{dt} = -\sum_{m'}\frac{\Gamma_{mm'}^n}{2}e^{i\omega_{mm'}t}a_{m'}(t), \tag{13}$$

with

$$\Gamma_{mm'}^n = \frac{\omega_{m'n}^3|d_{mn}d_{nm'}|}{3\pi\varepsilon_0\hbar c^3}. \tag{14}$$

Finally, if we allow for multiple levels on the right, this is the same as saying that there are multiple decay channels and one simply add the decay rates. Hence, the most general first-order differential equation governing the amplitude of the electrons on the left is

$$\frac{da_m(t)}{dt} = -\sum_{m'}a_{m'}(t)e^{i\omega_{mm'}t}\sum_n\frac{\Gamma_{mm'}^n}{2}. \tag{15}$$

3 | CALCULATIONS

3.1 | Model system

The above formalism applies very generally to describe the electron transfer from one material to another with

the emission of a photon. Each material can be an insulator, metal or semiconductor. In general, electron transfer between two materials could have a spin dependence from a spin-dependent potential. For the specific mechanism that we study in this work (optical emission), there is no dependence on electron spin and, therefore, magnetic properties except for its impact on spin-resolved band structures. Thus, our calculation applies to magnetic materials as well once the appropriate band structure is obtained.

For concreteness and simplicity, we report calculations for one-dimensional solids represented by finite linear chains of identical atoms. In order to allow for multiple bands and for band gaps, we use a two-band model for H_{elec} (Appendix). The resulting Wannier Hamiltonian for each material is then parameterized by a set of onsite and hopping parameters (Table 1). For simplicity, we have chosen the surface parameters to be the same as the bulk values. The tight-binding parameters for the left and right chains have been chosen to be very similar except for a rigid shift of the right energies down by 1 eV so that electrons can transfer between the same type of states from left to right with a loss of energy. We have also restricted the hopping to nearest neighbors.

We have carried out calculations for chains of various lengths. Example energy spectra for chains of 30 atoms are given in Figure 1. The bands are only quasi-continuous given the finite number of atoms; increasing the number of atoms leaves the allowed energy bands the same. Two bands are clearly visible and there are two almost degenerate surface states in the gaps (eigenstate labels # 30 and 31 in Figures 1 and 2). The decoupling of the left and right surface states gives an indication that the chains are long enough to simulate bulk properties; hence, we choose 30 atoms as the minimum chain length. States #32-35 are "band" states in the upper band.

We choose electrons in the left material to have a higher energy than those on the right and they can then transfer to the right material to occupy empty states there with the emission of photons. Since the photon emission process is governed by the strength of the dipole matrix elements, a model of the dipole transition strength between two eigenstates is needed. Equation (10) relates the band dipoles to atomic dipoles. A model of atomic dipoles was introduced in Reference 20. It is to be expected that the atomic dipole matrix element would weaken with the separation of the two atoms. Additionally, model calculations using hydrogenic orbitals reveal the dependence of the atomic dipole matrix elements with both atomic separation and with orbital type (Figure 3).

Hence, we have parameterized the distance (between the left and right materials) dependence of the atomic dipole matrix elements by a Gaussian function,

$$d_{i\alpha,j\beta}(x) = d^0_{i\alpha,j\beta} e^{-\gamma_{\alpha\beta}x^2}, \tag{16}$$

where we have chosen $\gamma_{\alpha\beta}$ to approximately reproduce the behavior displayed in Figure 3; we chose all $\gamma = 0.2$. We have kept optical transitions involving atoms that are up to two atomic sites apart (Table 2). For a two-level system, it is clear from Equation (14) that the decay rate is directly proportional to the strength of the dipole matrix element squared.

Finally, we have pointed out the importance of studying the temperature dependence as a way of getting insights into the charge transfer mechanism. Here, we assume that the effect of temperature is to change the electron distribution in the materials according to the Fermi-Dirac distribution:

$$f(E_m) = \frac{1}{1 + e^{\beta(E_m - E_F)}}, \beta = 1/(k_B T), \tag{17}$$

where E_m is the electron energy as before, E_F is the Fermi energy, and T the temperature. We assume that, at time $t = 0$ s and $T = 0$ K, electrons occupy all levels up to the Fermi energy.

TABLE 1 Tight-binding parameters (in eV)

	Left	Right
ε_s	−3.0	−4.0
ε_p	−5.0	−6.0
t_{ss}	−4.0	−4.0
t_{pp}	1.0	1.0
t_{sp}	−2.0	−2.0

3.2 | Results

We now present results of calculations of the charge transfer between two finite chains with the emission of photons. With M electrons on the left at time $t = 0$, the fractional charge transferred is calculated as

$$f_c(t) = 1 - \frac{1}{M}\sum_{m=1}^{M} |a_m(t)|^2. \tag{18}$$

Equation (13) is solved using the ode45 routine within MATLAB©; it uses the Runge-Kutta algorithm of order 4. Unless otherwise stated, all results will be for two

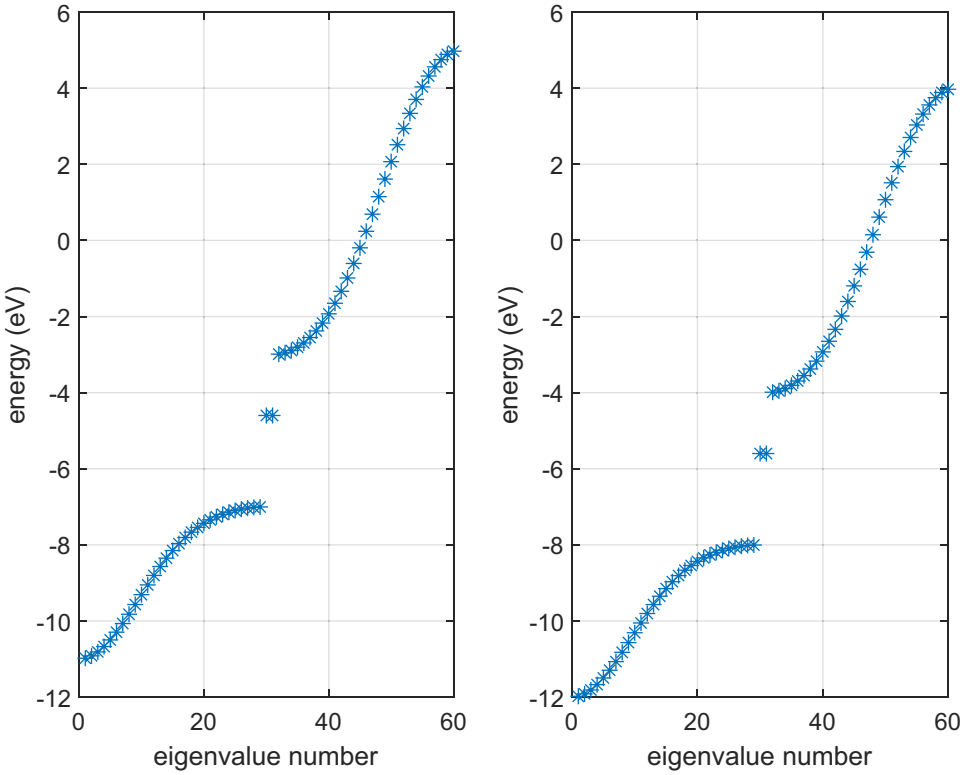

FIGURE 1 Energy spectrum of each atomic chain. Each chain has 30 atoms and 2 bands, with the onsite tight-binding parameters of the right chain shifted down by 1 eV

atomic chains of 30 atoms each, with no separation between the two chains, and at $T = 0$ K.

3.2.1 | Insulator-insulator

Consider first a two-level system, with one surface state occupied (eg, #30 in Figure 2) in the left material as the "excited" state and the other surface state empty (#31) in the right material. The fractional charging is shown in Figure 4. This is exactly the WW solution and the electron transfers from the left state to the right one at an exponential rate. One can introduce a measure of this charging rate as the time τ it takes to charge up to 63%; here, $\tau \approx 0.04$ μs. This is much slower than the quantum tunneling rate for isoelectronic charge transfer in References 21 and 22, where we obtained transfer rates in the femtosecond regime for a hopping parameter of the order of 1 eV. Hence, if the energy states in both materials are aligned, we expect quantum tunneling to be the dominant mechanism; otherwise, it is forbidden and the charge transfer can occur via photon emission. Both mechanisms require the contact spacing to be only a few Å (see below for calculations as a function of separation). Note, however, that while the transition is an electric dipole one and the rate is related to the dipole matrix element, the rate is also governed by the energy difference between the two levels (Equation (14)). Hence, for fixed dipole matrix elements, the rate increases with increasing energy spacing, that is, τ gets smaller. This is due to the larger phase space available for photon modes with increasing photon energy. Charge transfer between insulators has been postulated to involve surface states.[6] Hence, the above analysis could potentially apply to charge transfer between insulators.

3.2.2 | Insulator-metal

One can simulate charge transfer from an insulator to a metal by assuming the left chain to be filled up to the surface state and the right chain to have empty states in the lower band. Again, one can start with a two-level system if only one empty state is available; one obtains $\tau = 0.81$ μs. If there are more empty states available, one expects the decay rate to increase (see Equation (13)) and the decay time to decrease; indeed, assuming states #28 and 29 to be available, one finds $\tau = 0.17$ μs.

3.2.3 | Metal-Insulator

Our model of a metal is one with a partially filled band. Hence, we consider transitions from multiple levels in the upper band to the surface state. Consider the case with states #32-35 filled and decaying to state #30. The

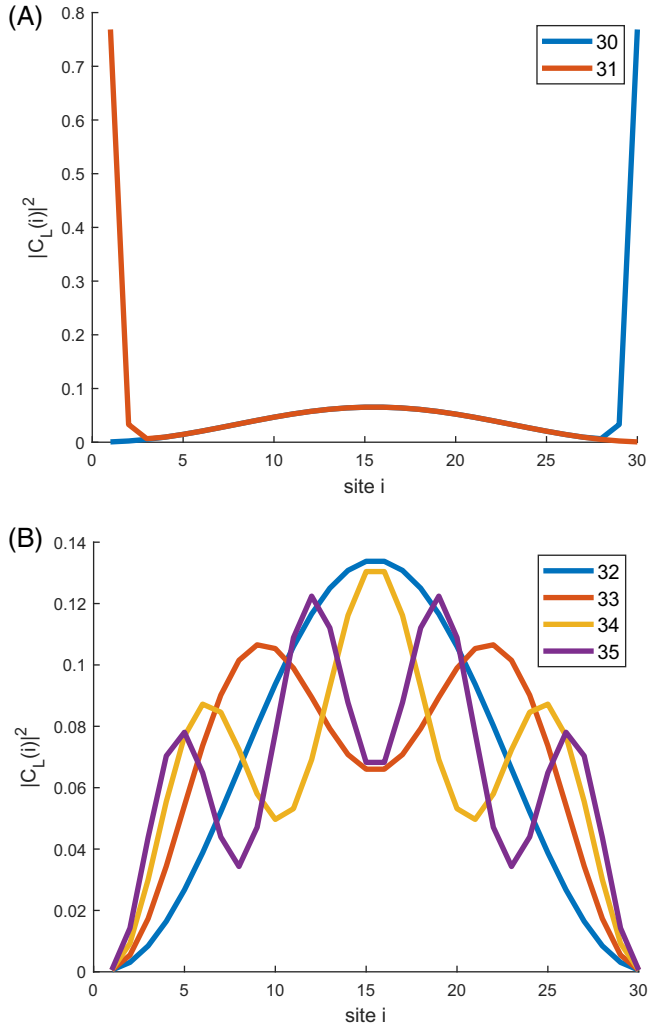

FIGURE 2 Wave functions of select states of an $N = 30$ chain, plotted as the coefficient squared at each atomic site. States #30 and 31 are surface states, each localized mostly at opposite surfaces, while states #32-35 are "band" states in the upper band

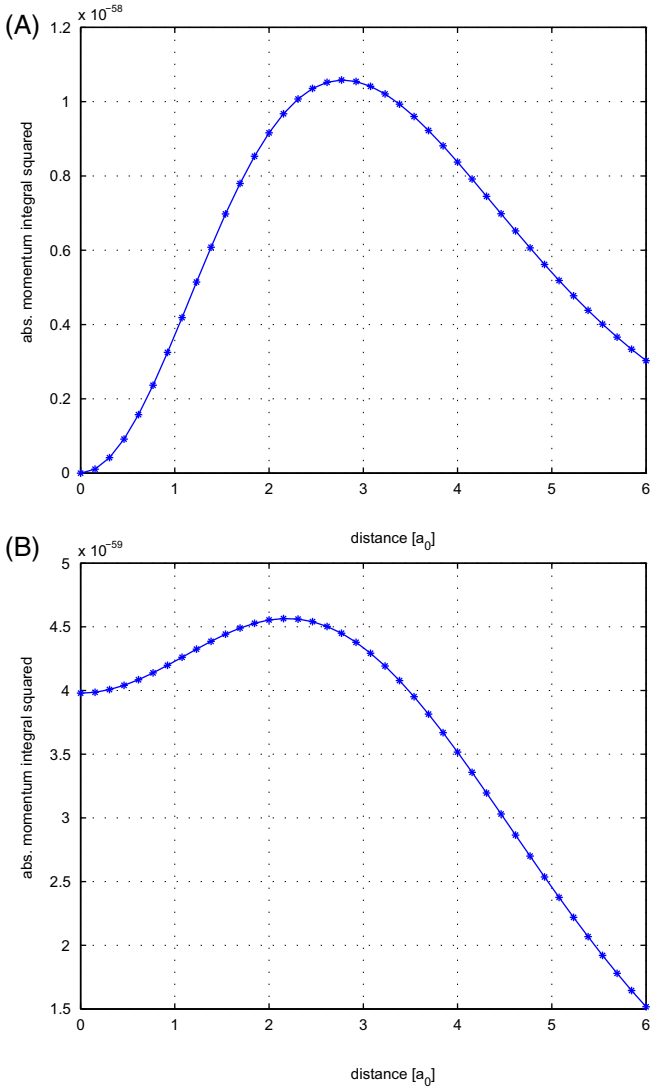

FIGURE 3 Model calculation of the squared absolute momentum integral as a function of atomic separation. Top: ss coupling, bottom: sp coupling

overall charging gives $\tau = 0.04$ μs (Figure 5A). Note, however, that one can compute the decay rate of each of the left states and they are different (Figure 5B). The difference in decay rate is due to both the different transition energies and different wave function localization. One sees in Figure 2 how the wave function "pushes" more toward the surfaces as the band index increases.

TABLE 2 Atomic dipole moments (in eÅ)

	d^0_{ss}	d^0_{sp}	d^0_{sp}
Nearest-neighbor	20.0	10.0	20.0
Next-nearest-neighbor	2.0	1.0	2.0

3.2.4 | Temperature dependence

There are a number of ways one can expect temperature to play a role in the charge transfer between two materials. One way is if phonons are emitted or absorbed in the process. However, we are not considering this additional mechanism in this article. Another is the change in the electronic properties with thermal expansion. This is known to lead to small changes in the band gap of a material of the order of a few tens of meV for a temperature change of 100 K. Since both materials will experience this effect, it will partially cancel out and the residual change in the energy difference between two states is likely insignificant. The more significant effect is expected to be a change in the electron distribution among energy states. However, the latter temperature

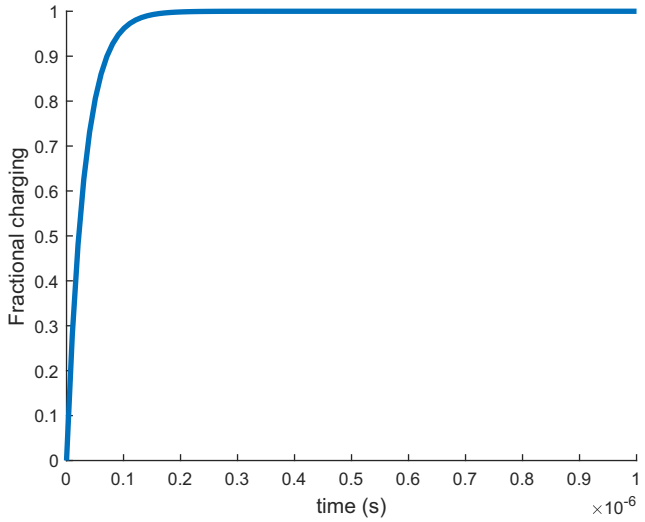

FIGURE 4 Fractional charging from one surface state to another for two atomic chains of 30 atoms each ($T = 0$ K)

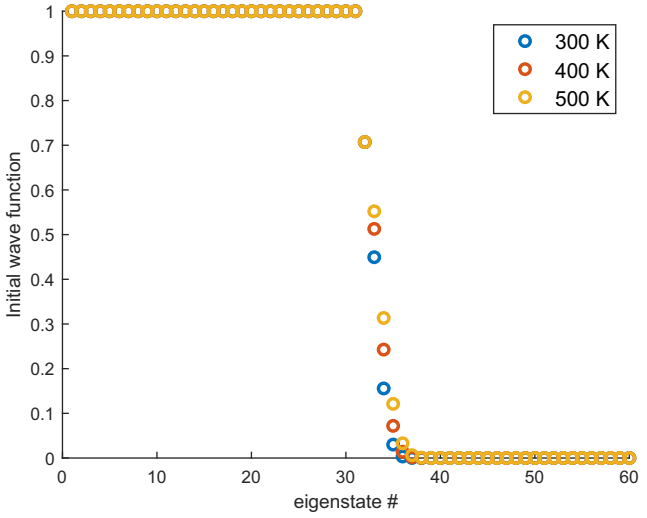

FIGURE 6 Initial state amplitude as a function of temperature: $T = 300$ K (blue circles), $T = 400$ K (red circles), $T = 500$ K (yellow circles)

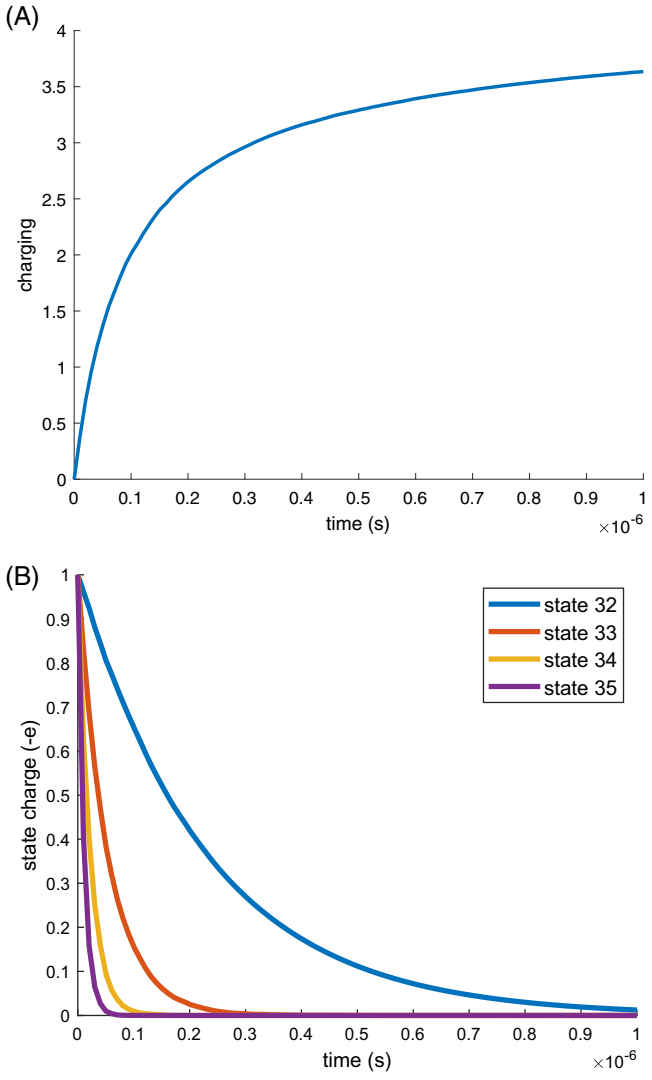

FIGURE 5 Charging from multiple states to a surface state for two atomic chains of 30 atoms each ($T = 0$ K). A, Fractional charging. B, Charge decay from each state

dependence is again expected to be negligible if the material is an insulator or even a semiconductor since the amount of electrons excited across a gap is very small even at room temperature. Indeed, we found this to be the case in our model when the uppermost electrons were located in the surface states.

Recent experimental data show an approximately linear increase of charge transfer of the order of 50% from 313 K to 433 K between a Au-coated AFM tip (metal) and a SiO_2 layer (insulator); that mechanism was attributed to thermionic emission and a lowering of the potential barrier for electron transport with increasing temperature. We consider here whether temperature can impact spontaneous emission. Indeed, for electrons originating from a metal, that is, when electrons do not completely fill a band, we did find some small changes in the transition rate. As an example, consider electrons populating all states up to the lowest upper band state (eigenstate #32) in the left material at $t = 0$ and for $T = 0$ K and transitioning to a surface state on the right (ie, an insulator). The change in that initial electron distribution as a function of temperature from 300 K to 500 K is shown in Figure 6. One can see some appreciable occupation of states higher than #32 for all three temperatures shown. Note that the energy difference between the lowest two upper band levels is about 36 meV for the 30-atom chain, hence the appreciable population at room temperature and above. At $T = 500$ K, states up to #35 have appreciable electron population (we used 1% as the cut-off). Thus, at finite temperatures, electrons from all these populated states can transfer to the right material with emission of photons. Since each of these states could have a different dipole matrix element and certainly a different energy compared to the state on the right, the transition rates are expected to be different.

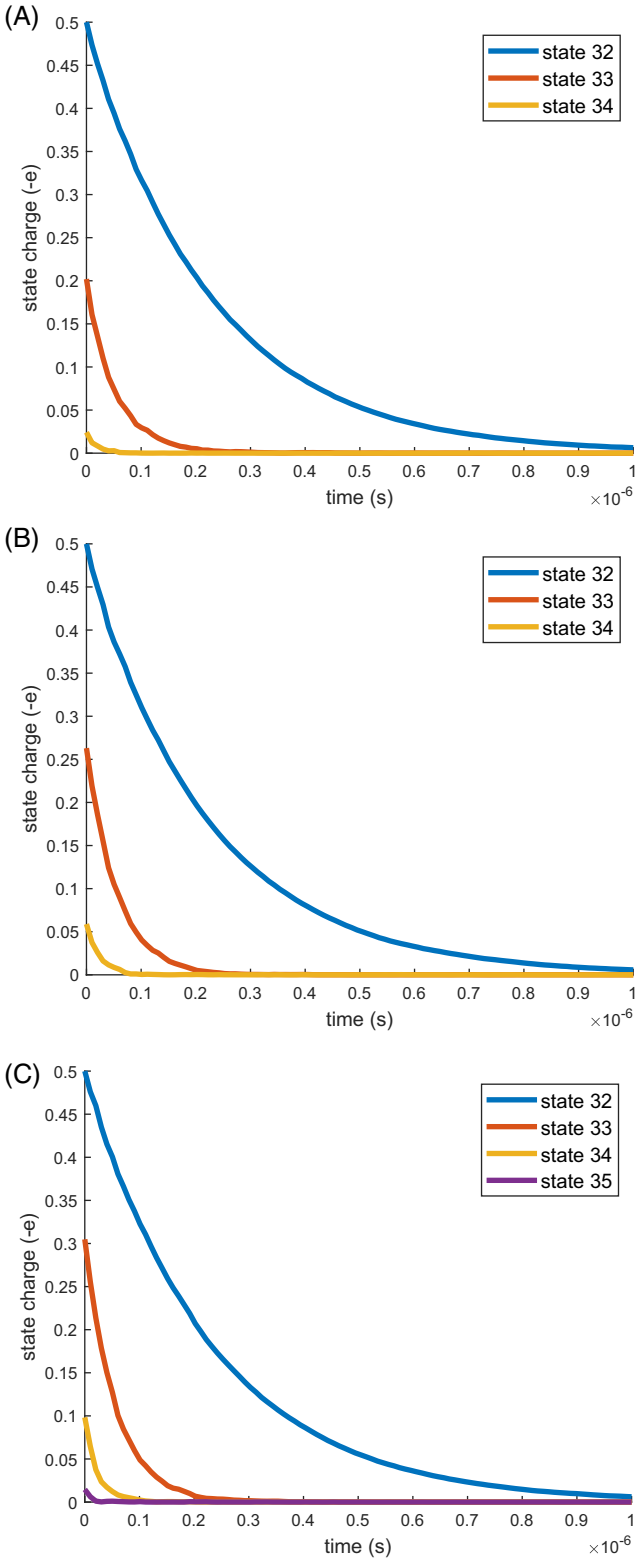

FIGURE 7 Change in population of individual states as a function of time. A, $T = 300$ K; B, $T = 400$ K; C, $T = 500$ K

An example of how the electron population in different states change with time for different temperatures is plotted in Figure 7. At $T = 0$ K (not shown), only states up to #32 are occupied; at $T = 300$ K and $T = 400$ K, there is appreciable occupation of states up to #34 and, for $T = 500$ K, state #35 is additionally occupied. We calculated the fractional charge transfer associated with these initial electron distributions (Figure 8). The different curves at different temperatures can be seen to be slightly changed, showing that there is some temperature dependence.

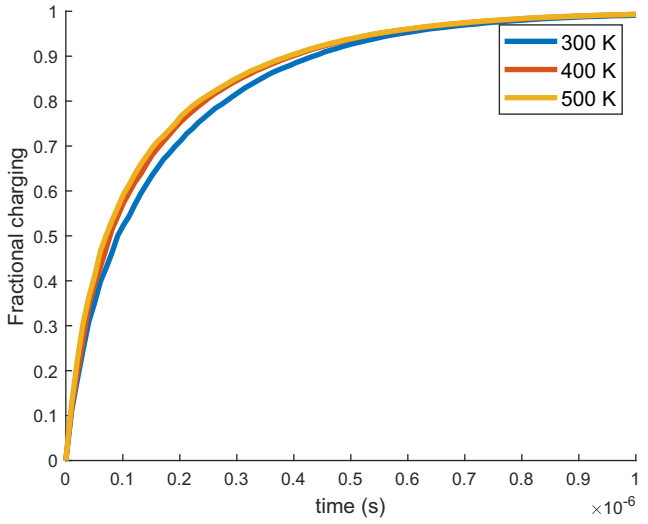

FIGURE 8 Fractional charging as a function of time and temperature (from $T = 300 - 500$ K). Assuming electrons are in eigenstates up to #32 on left (at $T = 0$ K) and transferring to eigenstate #30 (a surface state) on right

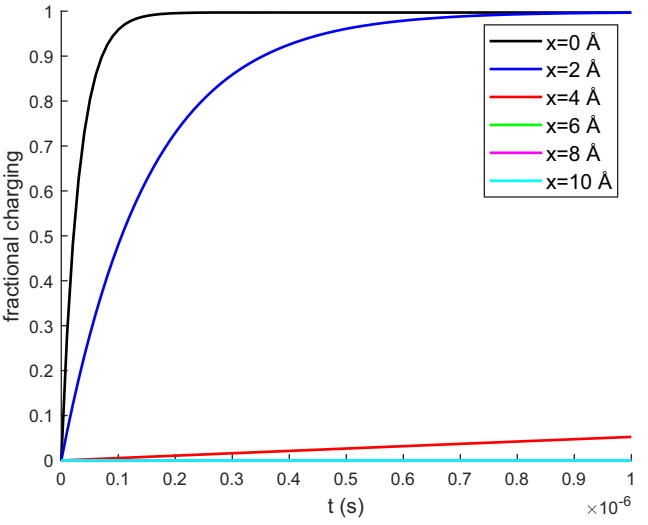

FIGURE 9 Charge transfer as a function of time for separations of 2 Å, 4 Å, 6 Å, 8 Å, and 10 Å beyond distance of closest approach ($T = 0$ K). Structure is two 30-atom chains with electrons transferring from a filled surface state to an empty one

3.2.5 | Separation

The charge transfer was also studied as a function of the separation of the two materials. One can identify the

possible physical reasons for a dependence from Equations (13) and (14). Note, first of all, that the electron wave functions and energies do not change since these are for each individual material. Hence, the only origin for a distance dependence lies in the atomic dipoles, as parameterized by Equation (16). For a two-level system (ie, isolated surface states on insulators), the overall decay constant is given by Equation (14), that is, it would decrease exponentially with the separation. A similar behavior should result for other systems. The results obtained at $T = 0$ K for separations from 0 Å (ie, touching) to 10 Å for an insulator-insulator contact is given in Figure 9. We illustrate with an example of the initial electron population filling the surface states on the left and available states on the right being the surface states. It can be seen that the charge transfer is strongly dependent on the separation. Indeed, there is no charge transfer for our model system for separations of the order of 5 Å. Hence, spontaneous emission is equally short-ranged as quantum tunneling is[21] in facilitating charge transfer between two materials.

4 | SUMMARY

The Weisskopf-Wigner model of spontaneous emission provides a physical picture of the process of thermoluminescence and has allowed us to analyze how the transfer rate of electrons depends on various factors such as the nature of the materials, their mutual separation and the external temperature. For electric-dipole allowed transitions, the typical decay time is in the range of microseconds. The charge transfer decays very quickly with increasing separation due to the weakening of the dipole transitions. Temperature is predicted not to be a factor for insulator-insulator contacts. Unless the system is enclosed in a cavity, the process is expected to not reach thermal equilibrium and to be irreversible.

ACKNOWLEDGMENTS

L.C.L.Y.V. acknowledges support from the Faculty Research Grant at the University of West Georgia. M.W. is grateful to the Talent 1000 Foreign Expert program for research funding.

ORCID

Morten Willatzen https://orcid.org/0000-0002-8215-9650

REFERENCES

1. Wang ZL, Lin L, Chen J, Niu S, Zi Y. *Triboelectric Nanogenerators*. Switzerland: Springer; 2016.
2. Wang AC, Wang ZL. On the origin of contact-electrification. *Mater Today*. 2019;30:34-51.
3. Kim S, Gupta MK, Lee KY, et al. Transparent flexible graphene triboelectric nanogenerators. *Adv Mater*. 2014;26:3918-3925. https://doi.org/10.1002/adma.201400172.
4. Hinchet R, Yoon H-J, Ryu H, et al. Transcutaneous ultrasound energy harvesting using capacitive triboelectric technology. *Science*. 2019;365:491-494. https://science.sciencemag.org/content/365/6452/491.full.pdf.
5. Yoon JH, Kim S-M, Eom Y, et al. Extremely fast self-healable bio-based supramolecular polymer for wearable real-time sweat-monitoring sensor. *ACS Appl Mater Interfaces*. 2019;11:46165-46175. https://doi.org/10.1021/acsami.9b16829.
6. Harper WR. *Contact and Frictional Dissipation*. Oxford: Clarendon Press; 1967.
7. Lacks D, Shinbrot T. Long-standing and unresolved issues in triboelectric charging. *Nat Rev Chem*. 2019;3:465.
8. Lacks DJ, Duff N, Kumar SK. Nonequilibrium accumulation of surface species and triboelectric charging in single component particulate systems. *Phys Rev Lett*. 2008;100:188305.
9. Mizzi CA, Lin AYW, Marks LD. Does flexoelectricity drive triboelectricity? *Phys Rev Lett*. 2019;123:116103.
10. Duke CB, Fabish TJ. Charge-induced relaxation in polymers. *Phys Rev Lett*. 1976;37:1075-1078.
11. Duke CB, Fabish TJ. Contact electrification of polymers: A quantitative model. *J Appl Phys*. 1978;49:315-321. https://doi.org/10.1063/1.324388.
12. Yoshida M. Experimental and theoretical approaches to charging behavior of polymer particles. *Chem Eng Sci*. 2006;61:2239-2248.
13. Shirakawa Y, Ii N, Yoshida M, Takashima R, Shimosaka A, Hidaka J. Quantum chemical calculation of electron transfer at metal/polymer interfaces. *Adv Powder Technol*. 2010;21:500.
14. Zhang Y, Shao T. Effect of contact deformation on contact electrification: a first-principles calculation. *J Phys D Appl Phys*. 2013;46:235304.
15. Shen X, Wang AE, Sankaran RM, Lacks DJ. First-principles calculation of contact electrification and validation by experiment. *J Electrostat*. 2016;82:11-16.
16. Lin S-q, Shao T-m. Bipolar charge transfer induced by water: experimental and first-principles studies. *Phys Chem Chem Phys*. 2017;19:29418-29423.
17. Wu J, Wang X, Li H, Wang F, Yang W, Hu Y. Insights into the mechanism of metal-polymer contact electrification for triboelectric nanogenerator via first-principles investigations. *Nano Energy*. 2018;48:607-616.
18. Wu J, Wang X, Li H, Wang F, Hu Y. First-principles investigations on the contact electrification mechanism between metal and amorphous polymers for triboelectric nanogenerators. *Nano Energy*. 2019;63:103864.
19. Alicki R, Jenkins A. Quantum theory of Triboelectricity. *Phys Rev Lett*. 2020;125:186101.
20. Willatzen M, Lin Wang Z. Theory of contact electrification: optical transitions in two-level systems. *Nano Energy*. 2018;52:517-523.
21. Willatzen M, Wang ZL. Contact Electrification by Quantum-Mechanical Tunneling. *Research*. 2019;2019:6528689.
22. Willatzen M, Lew Yan Voon LC, Wang ZL. Quantum Theory of Contact Electrification for Fluids and Solids. *Adv Funct*

Mater. 2020;30:1910461. https://doi.org/10.1002/adfm.201910461.

23. Xie Y, Li Z. Triboluminescence: Recalling Interest and New Aspects. *Chem*. 2019;4:943.
24. Weisskopf V, Wigner E. Berechnung der natürlichen Linienbreite auf Grund der Diracschen Lichttheorie. *Z Physik*. 1930;63:54-73.
25. Lew Yan Voon LC. *Electronic and optical properties of semiconductors: A study based on the empirical tight binding model*, PhD, Worcester Polytechnic Institute, Worcester, Massachusetts; 1993.
26. Allen L, Eberly JH. *Optical Resonance and Two-Level Atoms*. New York: Dover; 1987.

How to cite this article: Lew Yan Voon LC, Hasbun JE, Willatzen M, Wang ZL. Generalized Weisskopf-Wigner model of triboelectroluminescence. *EcoMat*. 2021;1–11. https://doi.org/10.1002/eom2.12086

APPENDIX: TWO-BAND, NEAREST-NEIGHBOR, FINITE CHAIN

We provide here the explicit form of the Wannier Hamiltonian given formally in Equation (2). We have assumed two orbitals on each atom (labeled as s and p-like), only kept nearest-neighbor interactions, and not assumed any periodicity. Projecting onto a space of atomic orbitals, the Hamiltonian matrix for N atoms is

$$\langle i\alpha|H|j\beta\rangle = \begin{pmatrix} & 1s & 1p & 2s & 2p & 3s & 3p & \cdots & & & (N-1)s & (N-1)p & Ns & Np \\ 1s & \varepsilon'_s & 0 & t'_{ss} & t'_{sp} & 0 & 0 & \cdots & & & 0 & 0 & 0 & 0 \\ 1p & 0 & \varepsilon'_p & t'_{ps} & t'_{pp} & 0 & 0 & \cdots & & & & & & \\ 2s & t'_{ss} & t'_{ps} & \varepsilon_s & 0 & t_{ss} & t_{sp} & \cdots & & & & & & \\ 2p & t'_{sp} & t'_{pp} & 0 & \varepsilon_p & -t_{sp} & t_{pp} & \cdots & & & & & & \\ 3s & 0 & 0 & 0 & -t_{sp} & \varepsilon_s & 0 & \cdots & & & & & & \\ 3p & 0 & 0 & t_{ss} & -t_{sp} & 0 & \varepsilon_p & \cdots & & & & & & \\ & & & & & & & \cdots & & & & & & \\ (N-1)s & & & & & & & \cdots & t_{ss} & t_{sp} & \varepsilon_s & 0 & t''_{ss} & t''_{sp} \\ (N-1)p & & & & & & & \cdots & -t_{sp} & t_{pp} & 0 & \varepsilon_p & t''_{ps} & t''_{pp} \\ Ns & & & & & & & \cdots & 0 & 0 & t''_{ss} & t''_{ps} & \varepsilon''_s & 0 \\ Np & & & & & & & \cdots & 0 & 0 & t''_{sp} & t''_{pp} & 0 & \varepsilon''_p \end{pmatrix} \tag{A1}$$

The parameters of the model are:

- Surface: $\varepsilon'_s, \varepsilon'_p, t'_{ss}, t'_{sp}, t'_{ps}, t'_{pp}$; $\varepsilon''_s, \varepsilon''_p, t''_{ss}, t''_{sp}, t''_{ps}, t''_{pp}$.
- Interior: ε_s, ε_p, t_{ss}, t_{pp}, t_{sp}.

In the current work, we have assumed for simplicity that all surface parameters are numerically the same as interior ones and chosen the remaining parameters as given in Table 1.